Novel Boundary Conditions for turbulent flows enclosed by porous media

Arpiruk Hokpunna[1*], Barbara Wohlmuth[2], Somchai Wongwises[1]

[1] Department of Mechanical Engineering, Faculty of Engineering, King Mongkut's University of Technology, Bangkok, Thailand 10140

[2] M2 - Zentrum Mathematik, Technische Universitaet Muenchen, Garching, Germany 85748

* Corresponding Author: Tel: +66-2-4709264, Fax: +66-2-4709111,

E-mail: arpiruk.hok@kmutt.ac.th

Abstract

In this paper we present the new boundary conditions for the turbulent flows enclosed by porous medium. Such flows play a crucial role in many areas such as filters, oil wells, heat exchangers, catalytic reactors, ground water pollution, scouring and deposition of pollutions at river bed. Since the porous media always consist of multi-scale structures starting from the dimension of the porous medium itself down to pore scale. Resolving all of these structures is too expensive considering the uncertainty of the porous media geometry representation. Under certain conditions, the effects of the porous media to the turbulent flows can be modeled as boundary conditions. However, the approach adopted in [1], [2] and [3] lacks some physical property of the flow at the porous media interface because in those works, either the slip velocity or the interface-normal velocity is assumed zero. The boundary conditions proposed in this work, are validated against the pore scaled simulation in which the whole porous media are resolved. The proposed boundary conditions deliver excellent normalized mean velocity and fluctuations. The numerical simulation using boundary conditions only uses 0.92 Million grid cells and it is computed on a simple workstation compared to 230 Million grid cells of the pore scaled simulation which is computed on a cluster with 512 nodes. The proposed boundary conditions allow accurate predictions of such flows to be accessible by the computing resources available in Thailand.

Keywords*:* boundary conditions, turbulent flows, direct numerical simulations, flow over porous interface, multi-physics

1. Introduction

Transport phenomena at the interface between porous medium and free flow play a crucial role in many areas. Filters, oil wells, heat exchangers, catalytic reactors, ground water pollution, benthic boundary layer are classic applications. In general, one can model the solid phase of a porous medium as an impermeable solid and solve the Navier-Stokes Equations (NSE) in the free flow part and in the void of the porous medium. It is possible to solve this problem with direct numerical simulation and obtain a full dynamic information of the flow. However, this approach is very expensive

especially when turbulent flows are involved. Together with uncertainty in the representation of the porous media, the accuracy of the prediction is unlikely to justify the cost of the simulation. Therefore, this problem are usually solved by two alternative strategies: (i) two domains and (ii) one domain approaches. In two domains approach, each domain is governed by its respective equation, for example NSE in the free flow and Darcy's Law in the porous media. In one domain approach, the whole system is considered to be a single continuum and the Volume-Averaged Navier-Stokes equations (VANS) [4] are used to solve in both domains.

On the other hand, if the coupling between these two domains is local and the main interest is the fluid side, the porous media can be removed from the computation and we can model the effects of the interface by a certain set of boundary conditions. This third approach is thus called boundary conditions approach and the interface of the porous medium is modeled as a porous wall. The investigation of fluid flow above porous layer has a long history. The early investigation of the modern days started in the 60s and most of the studies were concentrated on Stokes' flows (see [5,6 and 7]).

This is partly due to the earlier interests are focused on ground water flows. Only recently, the focus starts to shift to the Navier-Stokes equations such as [8, 9, 10 and 11] among others. In many situations, the flow in this coupling system can become turbulent and the validity of the tools developed for Stokes flows are thus can be questioned.

There are two boundary conditions proposed for permeable wall. The first approach by Jimenez et al. [1]. They proposed that for a porous medium with low porosity, the tangential velocity can be neglected and the interface-normal velocity can be computed from Darcy law. The conditions read

$$u = v = 0 \text{ and}$$
$$w = -\beta p'$$

where u, v and w are the velocities in the sreamwise, spanwise and interface-normal directions, respectively. These condition math with perforated surface such as those aiming at controlling fluid flow on airfoil. The second approach [2] assumes that follows similar concept of Beavers-Joseph conditions [5] in combination with Darcy law. These conditions read

$$\left.\frac{\partial u}{\partial z}\right|_{wall} = \frac{\alpha}{\sqrt{k}}(u_{wall} - Q),$$
$$\left.\frac{\partial v}{\partial z}\right|_{wall} = (v_{wall} - Q) \text{ and}$$
$$w = 0.$$

This approach assumes that there is no mass flux across the interface. These two approaches are on the extreme ends. One end assumes no flow in the normal direction, and the other end assumes now flows in the tangential direction. For typical porous media, fluid can flow in every direction. It is thus necessary to conduct a detail study on the relationship between the flow condition above and at the porous interface. The information from this study can then be used to construct a new type of boundary condition.

This paper aims at investigating the relationship between the flow conditions just above the porous media and the conditions at

the interface. To this end, we use direct numerical simulation of a turbulent flow above fully resolved porous media. We then present a novel boundary condition for turbulent flow enclosed by porous medium. These boundary conditions allow prediction of the mean flow and its fluctuation at a much lower cost in comparison to the fully resolved simulation where the flow inside the porous media is simulated. The paper is organized as follows. First, the setting of the direct numerical simulation where the new boundary conditions

2. Setup of fully-resolved simulation

The model porous media used here consists of eleven layers of the representative element in vertical. This number has been chosen desperately to ensure that the flow on the bottom part of the porous media is approximately laminar.

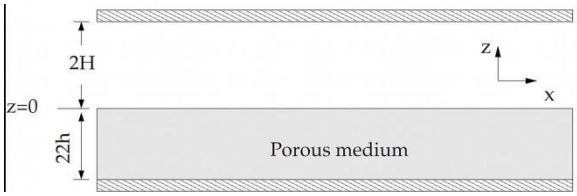

(a) Schematic of computational domain

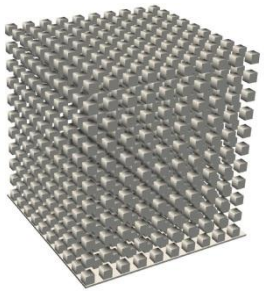

(b) A part of porous medium used in the experiment. This part is 20h×20h×22h in x, y and z.

Fig. 1 Setup of the numerical experiment.

In Fig.1 we display a group building blocks of the model enclosing the bottom domain over 10D×10D area on the streamwise-spanwise plane. Note that we do not consider sub-pore-scaled roughness, e.g. irregularities on the surface of the grain. Consequently, all surfaces of these cubes are treated as smooth no-slip walls.

The dimension of the computational domains normalized by the channel half-width (H), together with the number of grid cells are listed in Tab.1. In order to compare the flow under a comparable conditions, we fixed the bulk flow Reynolds number (Re_H). This requires a higher driving pressure gradient for the porous case. The ratio of the driving pressure gradient of each simulation normalized by that of the smooth wall case (p_x/p_{x0}) is shown in the table. The computational domain for the smooth wall case is the same as the one used in [12] Smaller domains are used for the porous wall case due to the autocorrelation of the velocities from our previous study (on a larger domain) drop to zero well within the size used here. The number of the cubes representing the porous media grain is 1500 where each cubes is resolved by 1200 grid cell.

A similar configuration was also used in [13], but with a larger pore relative to the channel width. The size of the computational domain in term of the roughness height in these simulations is significant larger than previous studies e.g. [14, 15 and 16].

Numerical grids are listed in Tab.1 along with the numerical grid for turbulent channel flow at Re = 5600 which is used as a reference test case to compare the effects of the bottom

porous wall. The grids used here are well smaller than the recommended values.

Table 1: Domain size and number of grid cells used in the simulations for porous media case (POR) and the reference smooth wall case (SMT).

Case	p_x/p_{x0}	L_x/H	L_y/H	N_x	N_y	N_z	$N \times 10^6$
Smooth (SMT)	1.00	12.56	4.20	256	160	144	5.9
Porous (PER)	2.20	4.91	2.95	1000	600	410	246.0

3. Numerical Approach

We solve the Navier-Stokes equations for incompressible Newtonian flows:

$$\frac{\partial u_i}{\partial x_i} = 0$$

$$\frac{\partial u_i}{\partial t} + \frac{\partial u_i u_j}{\partial x_j} = -\frac{1}{\rho}\frac{\partial p}{\partial x_i} + \nu\frac{\partial^2 u_i}{\partial x_j^2} + S_i$$

Navier-Stokes equations (NSE) are integrated within the standard framework of finite volumes method on staggered Cartesian grid. The spatial approximations are second-order accurate using centered interpolations and differentiations. Time integration is performed via a fractional step method with a third-order Runge-Kutta scheme. The pressure is obtained by a projection method at the end of each substep. The Poisson equation is solved by Stone's strongly implicit procedure (SIP). See [17] for a review on these standard methods. Detail information and accuracy of the code can be found in [18].

The pressure cells are positioned carefully such that the surfaces of the cubes coincide with the pressure cell and the region occupied by these cubes will be blocked from the computation. Since we use staggered grids, the momentum cells cannot be made aligned to the cubes surfaces. The effect of these solid surfaces to the momentum are represented by the immersed boundary method (IBM).The basic concept of our immersed boundary method is a functional fitting. A certain approximate function f(x,y,z) is assumed to represent the velocity field and boundary condition locally near the interpolating position. This function is determined by the method of undetermined coefficients.

Once the function is obtained, velocity components at a given point can be extracted. This gives a second-order smooth representation of the curved surface in our Cartesian grid.

In this work we use the cubic spline for the fitting function. Detail information about the immersed boundary method can be found in [19] The IBM used here have been used successfully in many turbulent flow investigations e.g. [20 and 21] among others.

4. Results for fully-resolved pore scale simulation.

In all cases, the flow is driven by the a constant pressure gradient which is adjusted such that the Reynolds number based on the bulk flow velocity and the channel width $ReH = 2U_bH/\nu$ are approximately 5600. The flows are let to develop and balance themselves without further mass control mechanism. The computations are performed on NEC Nehalem cluster at High performance computing center Stuttgart. The number of processor used for the smooth- and the porous walls are 32 and 512, resprectively. The larger case took about a month to complete the simulation. The flow statistics have been sampled for the time period of 500 and $352H/U_b$ in the smooth-, rough- and porous walls. These are corresponding to 40, and 72 through flow. A snapshot from the simulation of porous wall case is shown in Fig.2 where an ejection of low momentum fluid (A) and an inrush of the high

energy fluid (B) from and into the porous medium, respectively.

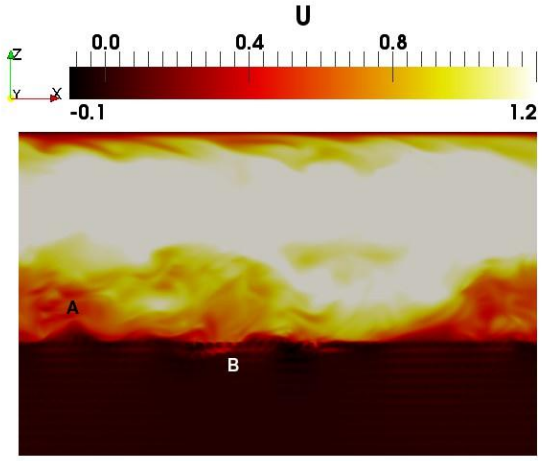

Fig.2: Snapshot of streamwise velocity showing ejection of low momentum fluid (A) and sweeping of high energy fluid (b).

4.1 Mean streamwise velocity

The overview of the mean streamwise velocity profiles sampled and averaged in time, streamwise and spanwise directions is displayed in Fig.3(a). The center of the channel flow with the porous wall is shifted closer to the top wall due to the higher skin friction at the bottom wall which requires a thicker boundary layer thickness (1.42H) to compensate. The boundary layer thickness here is measured from the nominal bottom wall (top of the cubes) to the point where the total shear stress vanishes. The mean streamwise velocity on the top (z=0) of the porous walls is $0.145U_b$. In Fig.3(b) we plot the normalized mean streamwise velocity profile without shifting the zero plane. The profile in the smooth wall case agrees well with the universal logarithmic profile. This is not the case for the boundary layer above the porous wall. In a usual boundary layer, the mean flow profile is consisting of viscous sublayer ($z^+<5$), buffer layer ($5<z^+<50$) and the outer layer ($z^+>50$). The region of the log-law usually starts from $z^+>30$ and spans to z/δ <0.3 before entering the wake region. The inflection point which is usually observed in the buffer region that connects the viscous sublayer and the log-layer are disappeared on the porous wall. It is still possible to fit the log law using $3.08\ln(z^+) - 7.34$ for $100<z^+<360$, but the power-law fit the profile on a lager range i.e. $7< z^+<360$.

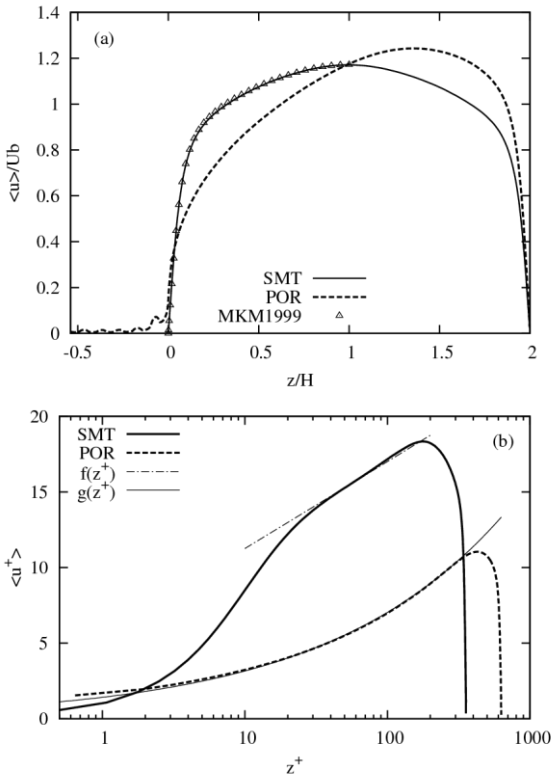

Fig.3: Mean velocity profile normalized by bulk flow velocity (a) and friction velocity at the bottom surface (b). The reference data from [12] is shown as MKM1999. The fitting functions according to the log-law and the power-law are $f(z^+) = 2.5\log(z^+) +5.5$ and $g(z^+) = 1.418\ (z^+)^{0.348}$, respectively.

4.2 Correlation of the interface condition and the condition at 1 z^+ above the interface

According to Beavers and Joseph [5], we know that, in laminar flow, the velocity is a continuous function, but the shear stress is not. To investigate the behavior of the volume averaged velocity and gradient in the vicinity of the surface under turbulent conditions, we plot the values averaged on the plane of the representative element volume (REV) and show them in Fig.4. The x-axis is the value sensed at 1 z^+ above the porous surface and the y-axis is the value at the interface. Note that REV is the smallest building block of the porous media. In this experiment it is the volume $8h^3$ enclosing the cubes. According to the figure, it is clear that the momentum at the interface is a linear function to the momentum at 1 z^+. The non-vanishing constant in Fig.4(a) is simply a result of the seepage flow within the porous media due to the driving pressure gradient which was applied throughout the domain. In Fig.4(b) the correlation passes the zero-coordinate which implies that, there will be now flow across the interface, if the flow is laminar. It is interesting to note that, the condition here is not exactly zero-gradient. Because, if it was the case, the flow coming into and out of the porous media will have to influence at all to the tangential components (due to mass-conservation). The shear stress, on the other hand, exhibits quadratic relation. It is important to note that, calculating the shear stress using the extrapolation from the information at the surface gives a broader scatter (larger error). This means the jump condition of Beavers and Joseph [5] is less accurate.

Having obtained the correlation of the conditions between the flow above and at the interface, we can proceed to the simulation where we remove the porous media from the computational domain and replace the effects of complex interaction at the interface by a simple set of boundary conditions. The result of this approach is presented in the next section.

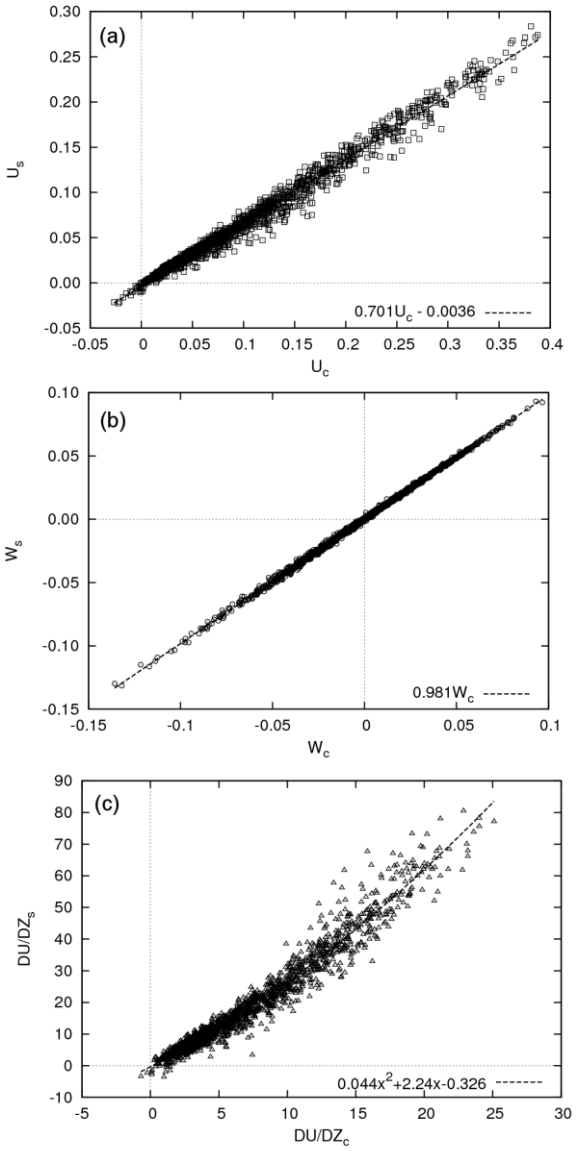

Fig.4 Correlation of the velocity and the streamwise velocity gradient at subsurface and the velocity at 1 z^+: (a) streamwise velocity, (b) wall-normal velocity and (c) streamwise velocity gradient in z-direction (du/dz). The x variable in (c) stands for du/dz.

5. Results from boundary condition approach

The goal of this study is to find the boundary condition which mimics the behavior of porous media surface. The final goal is that we can conduct DNS of fluid flow with porous medium at normal DNS grid resolution. For example, 6M grid cell instead of 246M grid cells. To evaluate the potential of this approach, we conduct a DNS of turbulent channel flow, driven by the same gradient as the POR case with the conditions obtained in the previous section. The computational domain in x, y and z is [6.28, 2.4, 2] with 0.9M grid cell. The simulation is conducted on 16 processor for 4 hours.

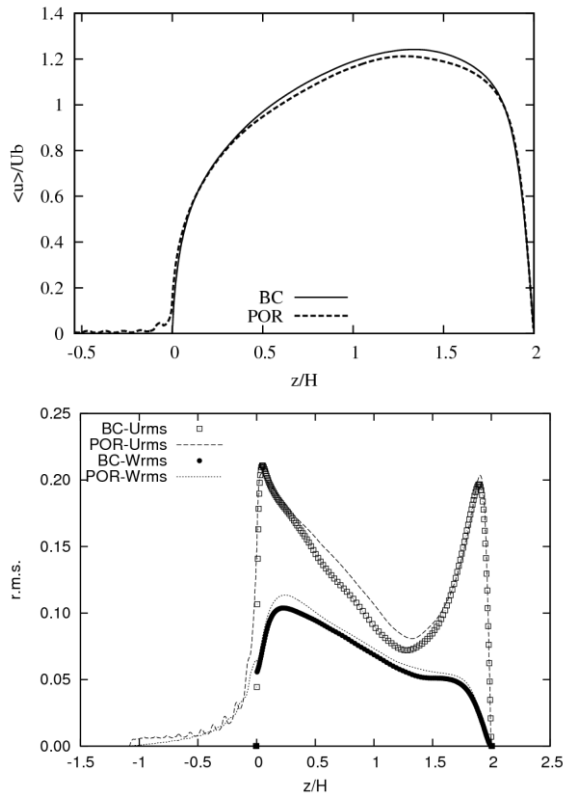

Fig.5 Mean streamwise velocity (top) and r.m.s. of velocity fluctuations (streamwise and wall-normal components) of the boundary conditions approach compared to pore-scale simulation.

The results in Fig.5(a) shows and excellent agreement between the boundary condition approach and the pore-scale simulation. Note that the boundary condition approach over predict the mass flow by 2.4%. A correction of this mass flow (scaling the plots) will bring the two curves on top of each other. The more interesting results are shown in Fig.5(b). The r.m.s. of the velocity fluctuations between two simulations are very close. This similarity indicates that the flow structures in these two simulations are quite similar.

6. Conclusion and outlook

Despite the huge different in grid resolution (273X) and the required computing resources, the boundary condition approach is able to predict the first- and the second-order statistics of the flow accurately. This new approach allows the studies to be conducted in Thailand where supercomputing facility is not available. The next step of the research in this direction is to find the dependency of the constant on the Reynolds number, pressure gradient inside the porous media and the channel.

7. Acknowledgement

The authors A. Hokpunna and B. Wohlmuth would like to thank the German Research Foundation (DFG) for financial support of the project within the Cluster of Excellence in Simulation Technology (EXC 310/1) at the University of Stuttgart.

8. References

[1] J. Jimenez, M. Uhlmann, A. Pinelli, and G. Kawahara, Journal of Fluid Mechanics (2001). Vol.442, pp. 89

[2] S. Hahn, J. Je, and H. Choi, Journal of Fluid Mechanics (2002). vol.450, pp. 259

[3] C. Wagner and R. Friedrich, Intl. Jour. of Heat and Fluid Flow (2002). vol.21(5), pp. 489

[4] S. Whitaker (1996), The Method of Volume Averaging, Springer Verlag.

[5] G. S. Beavers and D. D. Joseph, Boundary conditions at a naturally permeable wall, Journal of Fluid Mechanics Digital Archive (1967). vol.30

[6] P. Saffman, On the boundary condition at the surface of a porous medium, Stud. Appl.Math. (1971). vol.50(93).

[7] S. Whitaker, Flow in porous media I: A theoretical derivation of Darcy's law, Transport in Porous Media (1986). vol.1(3).

[8] M. Sahraoui and M. Kaviany, Slip and no-slip temperature boundary conditions at the interface of porous, plain media: Convection, International Journal of Heat and Mass Transfer (1994). vol.37, pp.1029.

[9] S. Whitaker, The Forchheimer equation: A theoretical development, Transport in Porous Media (1996). Vol.25(27).

[10] A. Shvidchenko. and G. Pender, Macroturbulent structure ofopen-channel ow over gravely beds, Water Resource Research (2001). vol.37, pp.709.

[11] D. Pokrajac, C. Manes, and I. McEwan, Peculiar mean velocity profiles within a porous bed of an open channel, Physics of Fluids (2007). vol.19, pp. 098109.

[12] Moser, Kim, and Mansour, Direct numerical simulation of turbulent channel flow up to Re=590, Physics of Fluids (1999). vol.11,pp. 943.

[13] W. P. Breugem, B. J. Boersma, and R. E. Uittenbogaard, The influence of wall permeability on turbulent channel flow, Journal of Fluid Mechanics (2006). vol.562, pp.35.

[14] K. Bhaganagar, J. Kim, and G. Coleman, E ect of Roughness on Wall-Bounded Turbulence Flow, Turbulence and Combustion (2004). vol.72, pp. 463

[15] T. Ikeda and P. A. Durbin, Direct simulations of a rough-wall channel flow, Journal of Fluid Mechanics (2007). vol.571, pp.235.

[16] O. Coceal, A. Dobre, T. G. Thomas, and S. E. BELCHER, Structure of turbulent flow over regular arrays of cubical roughness, Journal of Fluid Mechanics (2007). vol.589, pp.375.

[17] J. Ferziger and M. Peric, Computational Methods for Fluid Dynamics, Springer, 1996.

[18] M. Manhart, F. Tremblay, and R. Friedrich., Direct and large-eddy simulation of flow around a circular cylinder at subcritical Reynolds numbers, PhD thesis, Fachgebiet Strmungsmechanik, Technischen Universitt Mnchen, 2001.

[19] N. Peller, A. L. Duc, F. Tremblay, and M. Manhart, High-order stable interpolations for immersed boundary methods, International Journal for Numerical Methods in Fluids (2006)., vol.52, pp. 1175

[20] J. Gradl, H.-C. Schwarzer, F. Schwertfirm, M. Manhart, and W. Peukert, Precipitation of nanoparticles in a T-mixer: Coupling the particle population dynamics with hydrodynamics through direct numerical simulation, Chemical Engineering and Processing (2006). vol.45, pp.908.

[21] H. A. Khaledi, V. D. Narasimhamurthy, and H. I. Andersson, Cellular vortex shedding in the wake of a tapered plate at low Reynolds umber, Physics of Fluids (2009).vol. 21, pp.013603.